LUND UNIVERSITY

Laser-induced fluorescence in medical diagnostics

Andersson-Engels, Stefan; Johansson, Jonas; Svanberg, Katarina; Svanberg, Sune

Laser-induced fluorescence in medical diagnostics

Stefan Andersson-Engels[1], Jonas Johansson[1],
Katarina Svanberg[2], and Sune Svanberg[1]

[1] Department of Physics, Lund Institute of Technology,
P.O. Box 118, S-221 00 Lund, Sweden
[2] Department of Oncology and Department of Internal Medicine,
Lund University Hospital,
S-221 85 Lund, Sweden

ABSTRACT

We have performed extensive investigations using laser-induced fluorescence in animal as well as human tissue in order to localize diseased tissue and thus discriminate such tissue from normal surrounding areas. In characterizing different tissue types the endogenous fluorescence *(autofluorescence)* as well as specific fluorescence from different photosensitising substances was utilized. We have investigated different experimental and human malignant tumors *in vivo* and *in vitro* as well as atherosclerotic lesions *in vitro*. A fiber-optic fluorosensor was constructed and used in the experiments and in the clinical examination of patients. Dimensionless spectroscopic functions were formed to ensure that the signals were independent of clinically uncontrollable variables such as distance variations, tissue topography, light source fluctuations and variations in detection efficiency. A multi-color two-dimensional imaging system was constructed for real-time imaging. The system was tested peroperatively and during standard examination patient procedures. Besides utilizing the time-integrated fluorescence signal we have also investigated the possibility of incorporating time-resolved fluorescence characterization.

1. INTRODUCTION

Sensitive techniques for medical diagnostic purposes for detecting and localizing different diseases are very important. In many cases early diagnosis is of great importance in the prognosis, such as early discovery of endobronchial and urinary bladder malignancies. Methods such as conventional X-ray investigations or more complicated techniques such as computer assisted tomography (CAT) scanning X-ray and nuclear magnetic resonance imaging (MRI) are not always able to reveal early thin malignant tumor sites although signs of severe disease have been found in cytological tests of sputum and bladder contents. In some types of human malignancies, if not found although known to be present, no alternative diagnostic tool is available until the tumor has grown large enough to be visualized. Laser-induced fluorescence (LIF) as an additional diagnostic tool may improve the probability of earlier discovery [1]. The method relies on the fact that different tissue types posses different spectral properties, thus enabling diseased areas to be

discriminated from normal surrounding tissue. We have performed investigations in experimental tumor systems as well as in human malignancies utilizing the endogenous fluorescence (*autofluorescence*) from the tissue as well as specific fluorescence from systemically administered sensitizers; in the human cases Dihematoporphyrin ether/ester (DHE) [2,3] and for animal experimental tumors a variety of different photosensitizers, such as Hematoporphyrin (Hp), different Hematoporphyrin derivatives (HpD and DHE), Benzoporphyrin derivative - Mono Acid (BPD-MA) and Tetrasulphonated Phthalocyanines (TSPC) with selective affinity to different types of tissue [4-9].

Apart from the diagnosis of malignant tumors LIF may be incorporated for guiding in the procedure of laser angioplasty, a field in which a remarkable development has ocurred during the last few years. Percutaneously performed laser angioplasty has opened up possibilities for easy and convienient remodelling procedures of narrowed or obstructed vessels also for patients in a poor general condition which excluded them from major surgical procedures. Laser angioplasty utilizing a Nd:YAG laser has successfully been used in large, peripheral arteries giving as good results as surgical procedures in which the vessels have been replaced with artificial graft materials [10-13]. Also, excimer laser ablation has recently been used in peripherical artery remodelling [14]. Very recently, interest has been focussed on the possibility of treating atherosclerotic lesions in the coronary arteries by excimer laser ablation instead of open-heart surgery [15-17]. A reported complication utilizing laser angioplasty in peripherical vessels has been perforation of the vessels. In cases of peripherical artery procedures this complication may not be severely damaging. However, in cases of coronary angioplasty such a complication must be avoided as it is very deleterious in the small heart arteries

Biliary and urinary stone laser lithotripsy is another emerging field in which LIF could be used in order to guide the treating laser probe, utilizing the spectral characterization of the different stones as signals for system action, thus avoiding treatment failure. We have performed *in vitro* studies of different human kidney stones and ureter tissue, revealing variations in the spectral shape of the different stones and of the ureter wall [18].

In the present paper we will review the results obtained by our group in the field of tissue diagnostics using laser-induced fluorescence and also give references to related work.

2. INSTRUMENTATION FOR POINT MEASUREMENTS

In most of our studies a nitrogen laser emitting 3 ns light pulses at 337 nm was employed alone or in conjunction with a dye laser. We also used an excimer laser at 308 nm (XeCl) and an excimer-pumped dye laser. In the laboratory investigations the excitation light was directed to the sample by means of mirrors and the resulting fluorescence light was collected by an optical set-up of mirrors and lenses. The fluorescence light thus captured was directed onto the entrance slit of a polychromator, in which the light was dispersed and measured by a diode array. The spectrum was recorded from about 300 to 700 nm. A gated image intensifier was used in front of the diode array in order to increase the sensitivity. Spectra could be analysed in a computer.

In the clinical measurements and also lately in our experimental studies a more flexible fluorosensor was employed [19]. The excitation laser light is

focused into a 600 μm thick optical fiber which can be sterilized when used in surgical procedures or used through the biopsy channel of an endoscope. The fluorescence light is captured through the same fiber separated from the excitation light by a dichroic mirror. The fluorescence light is focussed onto the slit of the multichannel analyzer system. The fluorosensor is constructed as a mobile system and can easily be transported between different clinics.

For the time-resolved measurements a mode-locked argon-ion laser was used for synchronous pumping of a cavity dumped dye laser [20,21]. The length of the laser pulses was measured by an intersecting beam autocorrelator. The pulses had a pulse width of 6 ps. A dye laser was used to tune the argon-ion laser light to 674 nm in order to give light at 337 nm after frequency doubling. The repetition rate of the cavity-dumped laser was 6 MHz. A microchannel plate detector was used for time-correlated detection on individual photons. The fluorescence decay curves were recorded in a multichannel analyser and transferred to a computer for further evaluation.

In another system exploiting time resolution a short-pulse nitrogen laser in conjunction with a dual channel boxcar integrator was used to record the signal in different time intervals in the fluorescence decay. The detector was a photomultiplier tube used with a 380 nm interference filter. One detection channel captured the fluorescence at 5-15 ns while the other one detected the period 0-5 ns. The ratio between the two time intervals was formed in the boxcar system.

3. LASER-INDUCED FLUORESCENCE AND PHOTODYNAMIC ACTION IN MALIGNANT TUMORS

When UV-laser light is aimed onto biological tissue, large molecules absorb the light and give rise to a broad fluorescence distribution with the maximum in the blue-green wavelength region. This broad distribution is the total autofluorescence from several tissue fluorophores, such as tryptophan with its fluorescence peak at about 350 nm, chromophores in collagen and elastin with fluorescence peaking at 380 nm, nicotinamideadenine dinucleotide (NADH) with the fluorescence peak at 470 nm and melanines with a broad fluorescence centered at about 540 nm.

If previous sensitization has been performed with intravenously distributed substances, such as HpD, DHE, BPD-MA or PC, a specific fluorescence signal outside the broadly distributed autofluorescence can be identified in the red wavelength region. In some cases the specific fluorescence has a dual-peaked signature with maxima at 630 and 690 nm (HpD and DHE) and other sensitizers have one fluorescence maximum at 700 nm (PC) or 690 nm (BPD-MA), measured after injection intravenously.

In clinical use different derivatives of hematoporphyrin have been used for some time in the diagnosis as well as in the treatment of malignancies. The light absorption profile of hematoporphyrin derivative is characterized by an absorption peak at 405 nm in the Soret band. In addition to this marked maximum other smaller peaks can be seen with the last one occuring at 630 nm. A schematic energy level diagram for HpD is shown in Fig. 1. Besides giving rise to a specific fluorescence when excited by UV light the HpD molecules can also be used in an energy transfer process. Light in the red wavelength region (630 nm) is preferred in this process because of better tissue penetration. In this process, energy is transferred from the excited HpD molecules to the

Figure 1. *The molecular basis for HpD fluorescence and photodynamical action. (From S. Svanberg, Physica Scripta 1989).*
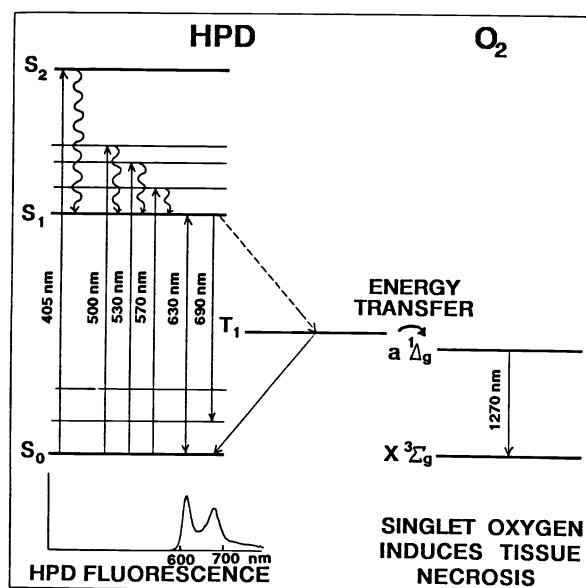
oxygen molecules in the tissue which are excited to singlet oxygen causing tissue necrosis. Oxidation of tissue due to free radical release can also eradicate malignant tissue sensitized with HpD. This process is called photodynamic therapy (PDT). Experience gained through the years is brought into Phase III studies aimed at palliative as well as curative treatment of a handful of different malignancies located in the airway tree, the oesophagus and the urinary bladder.

It has been proven that HpD-PDT is a promising treatment modality in a variety of types of thin malignant tumors, such as primary skin malignancies, cutaneously and subcutaneously located metastases and for *in situ* malignant lesions in the urinary bladder and in the bronchs [22-25]. Larger tumors cannot be treated with surface illumination as the 630 nm light does not penetrate deep enough. If thicker tumors are to be treated, interstitial treatment with optical fibers implanted in the tumor mass can be used. Another possibility is to apply surface illumination to the tumor bed after debulking the tumor mass. This kind of illumination is of special interest in connection with tumors which often recur locally. It has been tested for malignant brain gliomas in order to eradicate remaining tumour cells in the fresh tumor bed [26]. Other tumors of interest in this connection are malignancies in the pancreatic gland.

Another possibility would be to combine HpD-PDT with other treatment modalities. An interesting therapy combination for tumors thicker than 5 millimeters is PDT and light-induced hyperthermia utilizing light delivered through the same treatment fiber. Diode lasers can be utilized as a complementary light source. The use of frequency doubled Nd:YAG laser light for dye laser pumping to achieve PDT combined with the laser light at 1064 nm would be another possibility. Simultaneously delivered HpD-PDT and light-induced hyperthermia has been performed in our group to treat recurrent breast cancer. Although a primitive light delivery system for the hyperthermia part

of the treatment was used we succeed in eradicating tumors of a thickness of 20 millimeters [2,3].

At the Lund University Hospital it is planned to start a PDT program using dedicated laser equipment during early spring 1990 as a successor to our initial work [2,3]. In this PDT program, including five different clinics, the diagnostic work will also continue, utilizing our imaging system [27-29] which will be described more extensively below.

4. AUTOFLUORESCENCE IN MALIGNANT TUMORS

In our early work using LIF in detecting malignancies, we observed some useful characteristics of the autofluorescence signal. On comparing the fluorescence signals in the blue-green wavelength region originating from malignant and non-malignant tissue the intensity in the diseased area is seen to decrease. This phenomenon with decreased autofluorescence in the blue-green region was demonstrated for experimental tumor tissue as well as for human malignancies whether the normal undiseased surrounding tissue was muscle, skin or brain parenchyma. In some malignant tissue types specific signatures in the autofluorescence can also be seen outside the blue-green wavelength region which would increase the demarcation capability using only the endogenous fluorescence of malignant tissue.

Clinical recordings of tissue autofluorescence utilizing a fiber-optically equipped fluorosensor constructed and built at the Lund Institute of Technology [19] were performed in three different clinics at the Lund University Hospital. The investigations were done in connection with bronchoscopy of the airways, in standard tumor examination of the oral cavity and peroperatively when resecting malignant brain tumors. In the investigated bronchogenic tumors of different kinds the autofluorescence alone does not appear to be very promising in demarcating malignant tumors as the spectra do not show significant differences in spectral shape. The overall fluorescence intensity is, however, lower in the tumors compared with normal bronchial wall. In the case of malignant brain tumors, the spectral shape of the autofluorescence from normal brain compared with malignant brain tumors shows some interesting differences. In Fig. 2 we show that in a relatively small material, astrocytoma grades III and IV can be separated from lower grades of the tumor and normal brain parenchyma.

In the investigations of oral cavity malignancies we have been able to identify specific fluorescence in the red wavelength region. An example is shown in Fig. 3 where the signal at 630 nm probably originates from endogenous porphyrins retained in the malignant tumor area. The same observation has been made by Chinese researchers in human malignancies located in the oral cavity, in the stomach and in the gynecological sphere [30-33]. Some of the tumors investigated by the Chinese researchers were very thin lesions impossible to identify by standard examination methods but detected with UV-excited auto-fluorescence utilizing quite simple equipment. Biopsy specimens were taken from areas in accordance with the red autofluorescence signal, veryfying the malignant diagnosis.

ASTROCYTOMA
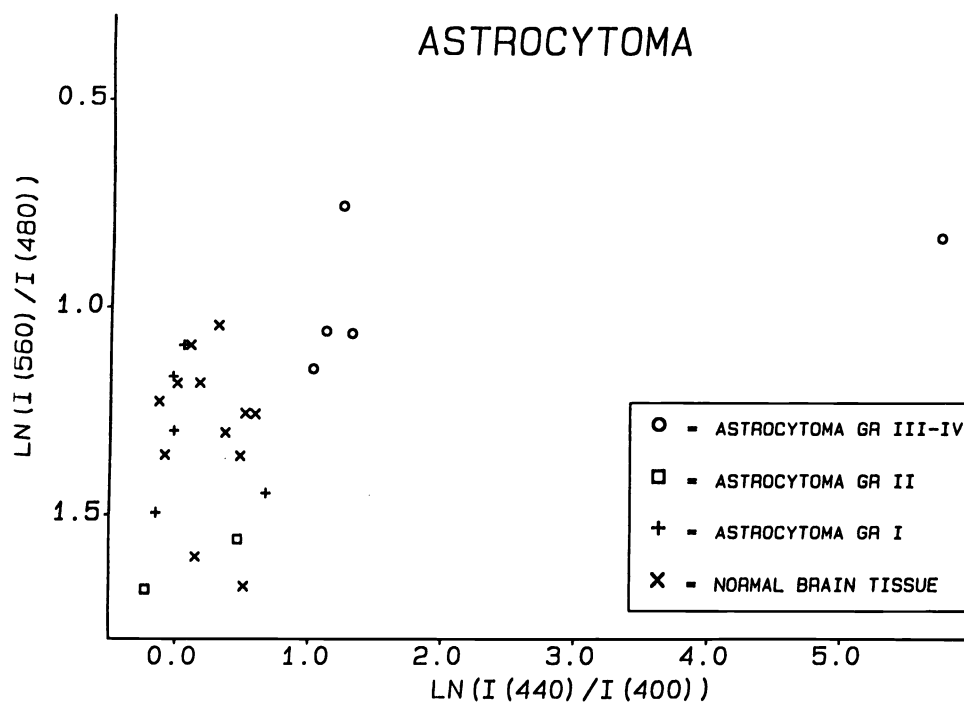
Figure 2. *A correlation diagram for two dimensionless functions LN(I(560 nm)/ I(480 nm))and LN(I(440 nm)/I(400 nm)) of four fluorescence intensities for 24 histopathologically classified brain tissue samples of normal brain and various malignancies. The excitation wavelength was 337 nm. (From Ref. [19]).*
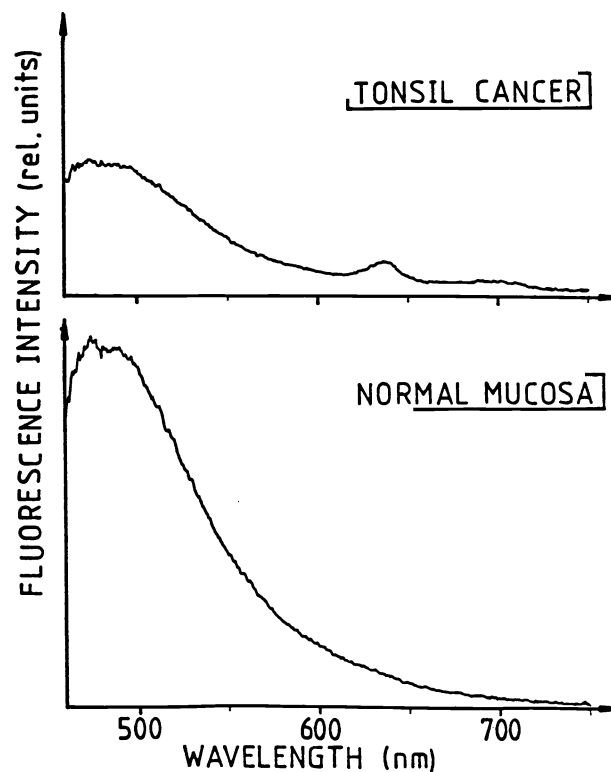
Figure 3. *In vivo fluorescence spectra from a tonsil cancer and the normal pharyngeal mucosa using 405 nm excitation light. (From Ref. [19]).*

5. CONTRAST ENHANCEMENT

When the clinically used sensitizers (HpD and DHE) are administered intravenously skin photosentitization lasting for about four weeks takes place parallel to the malignant tumor sensitization. This undesirable side-effect is known to be correlated to the drug dose given and if the dose could be lowered by a factor of 2-3 the problem would largely be avoided. For diagnostic purposes it seems to be possible to lower the drug dose and still localize malignancies by using the full spectral information available including the autofluorescence. As already pointed out, the autofluorescence in the region peaking at about 470 nm decreases in malignant tissue at the same time as the specific fluorescence signal in the red wavelength region increases. By dividing the fluorescence intensity at 630 nm by the autofluorescence intensity at 470 nm an enhanced contrast is obtained.

Figure 4. *Fluorescence data from a scan across a breast carcinoma metastasis 1 day after DHE injection. Sample spectra for tumor and normal tissue are shown with evaluated parameters indicated. The tumor is clearly demarcated in the A and B functions and especially well in the A/B function. (From Ref. [3]).*
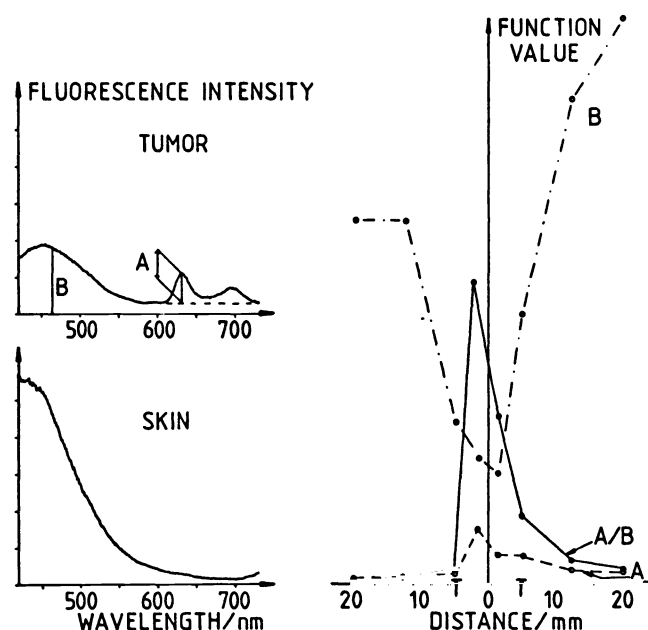
If the fluorescence signal in the red wavelength region is lifted off the background autofluorescence signal, on which it is superimposed, the contrast is enhanced [1,4-6,34-36]. This is illustrated in Fig. 4 showing fluorescence data for a metastasis of human breast carcinoma before PDT. Fluorescence spectra are shown for a basal cell carcinoma and the normal surrounding skin in a patient who had received DHE at a dose of 2.5 mg/kg b.w. 3 days earlier. The figure shows the decreased autofluorescence (marked B) in the tumor area and the increased signal at 630 nm (marked A). A scan was placed over the tumor region with normal surrounding skin. The tumour area is clearly demarcated by the signals A and B and especially well in the ratio A/B, illustrating the contrast enhancement obtained in this case. It is of special interest to note that the demarcation of the tumor area is stong although the surrounding tissue in this case is skin, which is known to be sensitized. After PDT was administered to the tumor area including small islands of normal skin in the lesion necrosis did not affect the normal skin, although the whole area was illuminated [2].

We have earlier showed a marked contrast enhancement in an experimental rat glioma using the reduced drug dose of 1 mg/kg b.w. DHE 24 hours prior to the investigation [8]. When dividing the background-free drug-related fluorescence signal by the autofluorescence signal a stong contrast enhancement of about 50 for the tumor area is obtained, although the drug dose was lowered by a factor of 2.5.

Besides providing the possibility of lowering the drug dose by utilizing this contrast enhancement, there are other advantages in using such ratios. The resulting simple function has no dimensions and variations in the excitation and detection efficiency can be neglected. Furthermore, the dimensionless contrast functions provide an immunity to surface topography and distance variations as the autofluorescence signal as well as the specific fluorescence signal emanating from the administered drug are affected equally. This is of special importance in endoscopic use with the illumination of an inhomogeneously shaped tumor in a breathing patient.

6. DEVELOPMENT OF NEW SENSITIZERS

As mentioned above, the concept of incorporating the endogenous fluorescence in the data processing for contrast enhancement would make it possible to lower the drug dose for diagnostic purposes, thus avoiding the unwanted side-effect of skin sensitization. Another possibility is to use more specific tumor-marking drugs with faster clearance. The search for the "perfect" photosensitizer has continued for many years and the properties which have to be fulfilled are many, such as exhibiting a fast metabolism, high tumor sensitivity and being as non-toxic as a substance can be. The property of the light absorption profile with strong absorption in the red and near IR wavelength region is also important. Almost all research work has stressed the point that a clinically useful photosensitizer has to fulfill the properties to suit diagnostic as well as therapeutic use. Maybe different drugs are needed for the two applications.

Recently, the porphyrin derivative BPD-MA has been produced exhibiting many attractive properties [37-40]. The substance is cleared from the living organism in 24 hours and has a selectivity for malignancies. It is also claimed by the producer to have a high fluorescence yield and to be photodynamically potent. The drug has a light absorption profile enabling the use of therapeutic light at about 680 nm, thus enabling treatment of larger tumors than with HpD and DHE.

We have performed some initial investigations in rats, detecting the fluorescence from different rodent tissue types including an experimental adenocarcinoma [9]. In Fig. 5 a LIF spectrum of the malignant tumor in a rat injected with 3 mg/kg b.w. BPD-MA is shown together with the evaluated data of a scan across the tumor area with surrounding healthy muscle on both sides. As seen in the figure the fluorescence signal from BPD-MA (marked A) is single-peaked with the maximum at about 690 nm. It is also seen that the demarcation in the A signal is about 2-3 for the tumor compared with the surrounding healthy tissue. If the autofluorescence is incorporated into the tumor discrimination criteria, the demarcation tumor to muscle is increased.

For the same experimental system we have also tested the tumor demarcation potential of Hp, the monomeric building block in HpD and DHE, [7] and found the demarcation ratio tumor to muscle to be about 2:1 with enhanced

Figure 5. *Fluorescence data from a scan across a tumor in the hind leg of a rat 3 hours after injection with 3 mg/kg b.w. BPD-MA. (From Ref. [9]).*
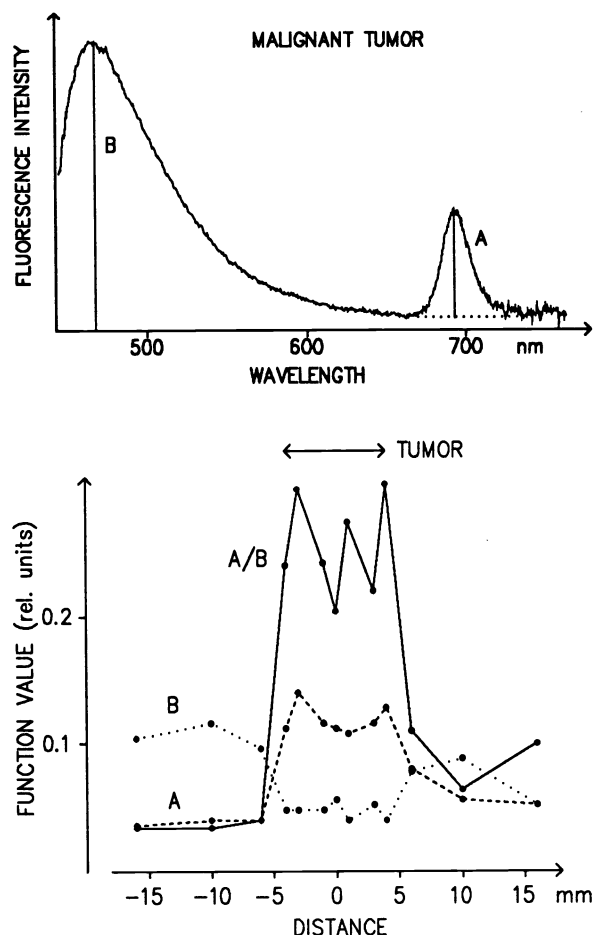

demarcation when including the autofluorescence. Hp as well as BPD-MA is known to metabolize very fast without sensitizing the skin. BPD-MA has to be dissolved in small amounts of DMSO (dimetylsulphoxide) before diluted in saline, while Hp is totally water soluble. It is an attractive idea if BPD-MA or Hp could be injected some hours before the diagnostic procedure, thus enhancing the possibility for the examining doctor to reveal early tumors without sensitizing the patient.

7. LASER-INDUCED FLUORESCENCE IN ATHEROSCLEROSIS

Atherosclerosis is a widespread disease known to cause a variety of adverse effects. Easy and convenient treatment modalities besides conventional surgical procedures are desirable and the development of percutaneous laser angioplasty is an interesting possibility. Parallel to this development a need has evolved for better diagnostic equipment to be used during the procedure, as some complications are known to occur, such as vessel perforation. Although angiography and ultrasound techniques have been improved, spectroscopic methods may be useful for detection of the detailed atherosclerotic lesions in the vessel wall. A feed back guiding system in the treatment procedure is desirable in order to avoid complications [41].

When the process of atherosclerosis starts in the artery vessel, the intimal layer of the wall is thickened and new constituents are deposited in the tissue. During the initial stage a fibrotic plaque develops with increasing amounts of collagen and elastine. Later in the process lipid droplets and cholesterol crystals are deposited. An inflammatory response can be identified with fagocytes and macrophages in the diseased area. Later, calcium is incorporated and sometimes the surface endothelium layer is damaged with thromembolic material on top of the damaged area. A schematic illustration of an atherosclerotic plaque in a vessel wall is given in Fig. 6.

Figure 6. *Illustration of a cross section through a blood vessel with an atherosclerotic plaque. A thrombosis is under development on the downstream side of the plaque. (From S. Andersson-Engels et al. Anal. Chem.1990).*
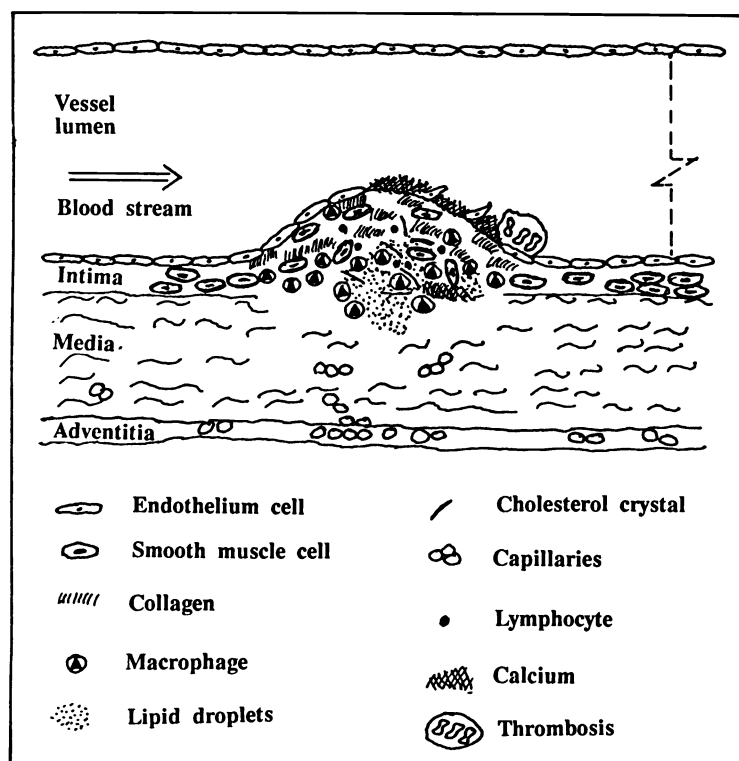
In demarcating atherosclerosis from the normal artery wall it has been shown by us and others that the autofluorescence alone can be used in demarcating diseased tissue as the spectroscopic signature from the normal artery wall is different compared with that of the atherosclerotically diseased one [42-51]. This is illustrated in Fig. 7 (upper part) with two typical fluorescence spectra from a plaque region and from a normal artery wall. We have seen in our investigations that the signature *in vitro* from a plaque region differs somewhat depending on the stage of the atherosclerotic process. The earlier fibrotic lesions can be separated from the plaque regions with higher fat content and also from calcified regions. We have been able to spectroscopically separate four different classes of plaques depending on the severity of the disease. This is illustrated in Fig. 8. Group I includes the least damaged tissue with only small amounts of fibrotic constituents. In group II more fibrotic constituents are present. Group III includes lesions with calcium content in the plaque, while in group IV calcium occurs at the surface. In this group (IV) the lesions with endothelium damage with or without thrombotic material on the damaged surface are included. The overall fluorescence intensity is heavily reduced in cases of endothelium damage.

Figure 7. *Laser-induced fluorescence spectra from normal and atherosclerotic plaque (at the top). The fluorescence intensities at five different wavelengths 390, 415, 480, 580 and 600 nm (denoted a - e) are indicated. Example of a scan through an athero-sclerotic plaque region with data from three dimensionless contrast functions is displayed at the bottom. (From Ref. [49]).*
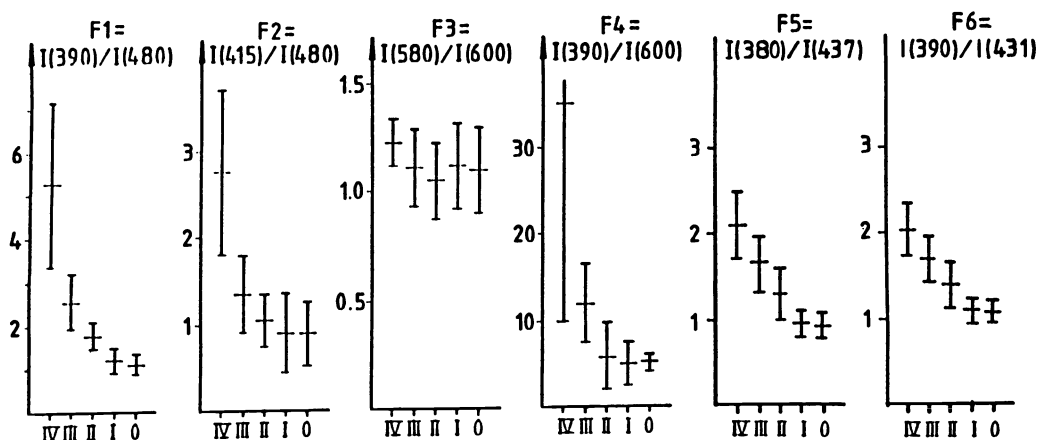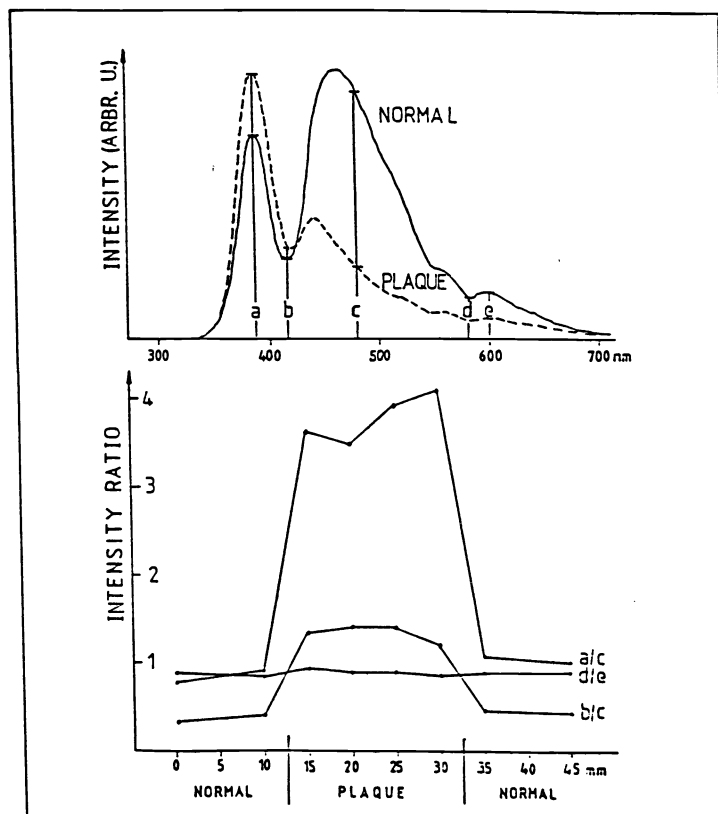

Figure 8. *Six dimensionless contrast functions for normal artery wall and four different groups of plaques (I-IV), ranked in accordance with the severity of the atherosclerotic damage. Data for F1-F4 are identical with those given in Ref. [49], while F5 and F6 represent blood-independent functions presented in Ref. [28]. (From Ref. [28]).*

Besides being characterized by the signature of the different chromophores in the tissue the fluorescence from vessel walls is also influenced by the hemoglobin in the blood content in the wall distributed via *vasa vasorum* and the blood inside the lumen of the vessel. Light transmission through arterial and venous blood is strongly wavelength dependent, as illustrated in Fig. 9. The transmission is very low at 420 nm and is also reduced at 540 and 580 nm. The fluorescence signal is correspondingly reduced due to reabsorption by the blood. In the figure wavelength pairs at which the blood absorption is equal are indicated. If the fluorescence is chosen at these wavelengths the differential absorption is zero and the influence of blood can be neglected. As seen in Fig. 7 both spectra are influenced by the absorption of hemoglobin with a marked minimum at about 420 nm and some smaller reductions at 540 and 580 nm.

Figure 9. *Transmission spectra through 0.2 mm thick layer of arterial (at the top) and veneous blood (at the bottom), both diluted in saline to 20% concentrations. Wavelength pairs of equal absorption are indicated. The blood samples were drawn from the same person. (From Ref [28]).*
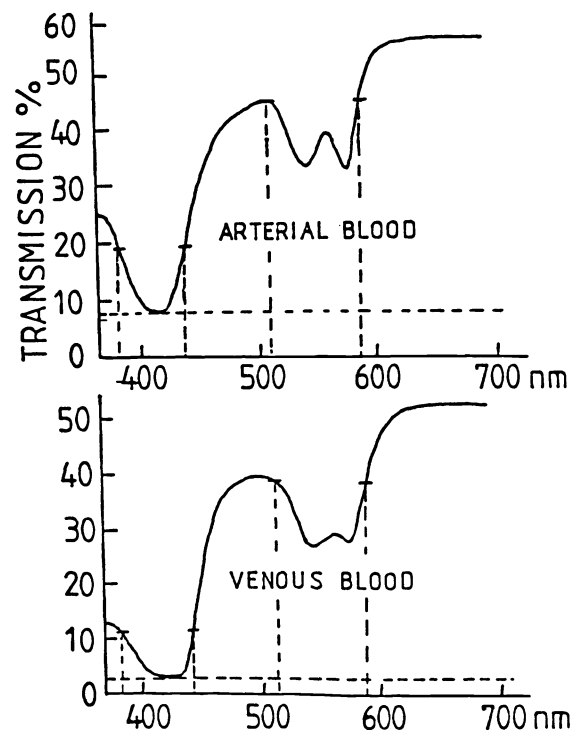
When investigating fluorescence from thin lesions it is important to use excitation light of a short wavelength in order not to penetrate deeper into the tissue than the process of the disease itself. We have used a pulsed nitrogen laser with light emission at 337 nm which is preferable compared with others who used excitation light at about 480 nm [42,43,47,51]. If the diagnostic light penetrates too deeply into the tissue the signal is diluted with information from non-diseased areas and the light reabsorption interacts with healthy tissue surrounding the area of interest. We have investigated the fluorescence signature from the different layers of the diseased and healthy artery wall following mechanical peeling apart of the different layers (Fig. 10). It seems that ·the deeper into the plaque region the signal is captured the more similar the signature is to that of undiseased areas. The most striking spectroscopic difference is seen in the layers at the inner surface of the lumen, endothelium layer and the intima, while the
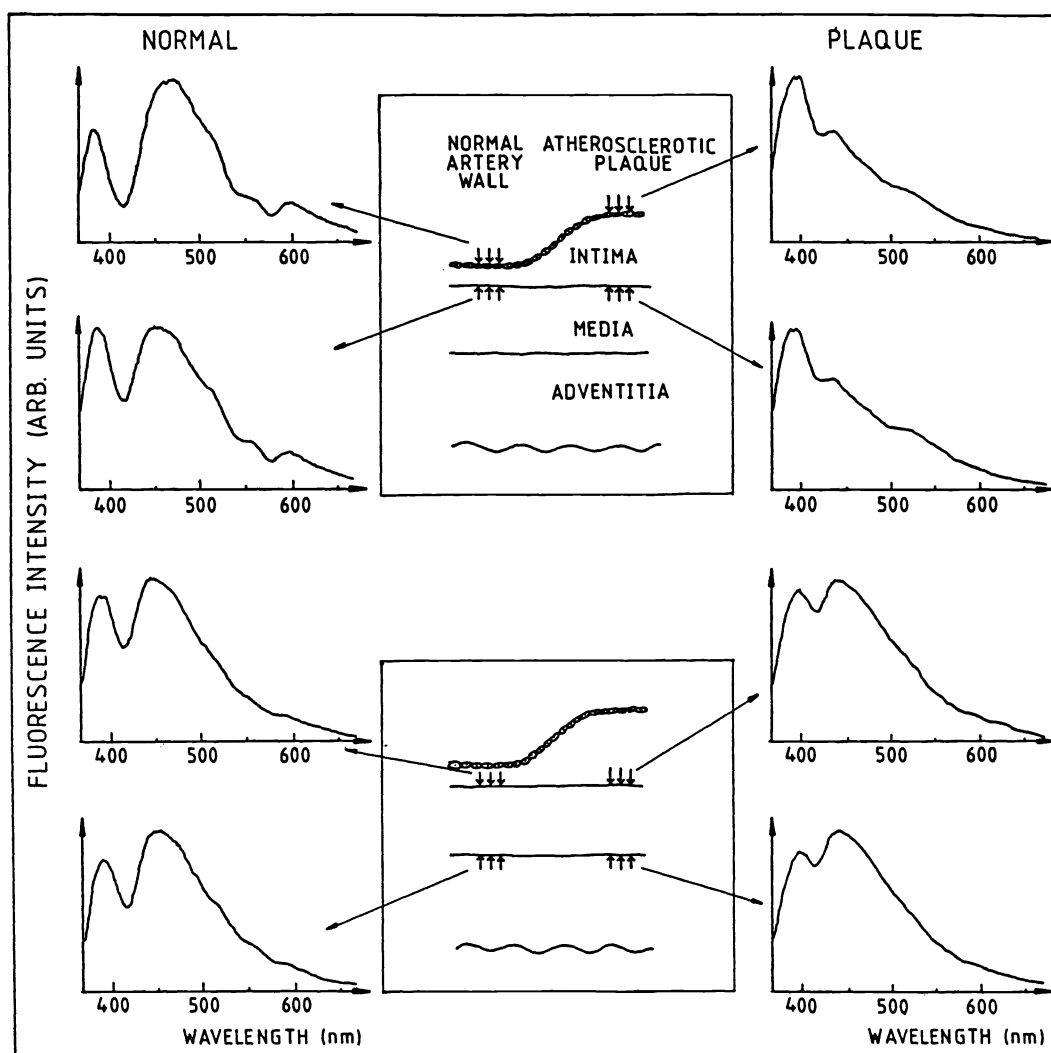
Figure 10. *Laser-indced fluorescence spectra of different vessel-wall layers. To the left in the figure the shapes of the distributions for the different layers in normal aortic vessel wall are shown, recorded with blocking aluminium foil between the layers. To the right in the figure the corresponding spectra for atherosclerotic aorta are given. (From Ref. [49]).*

spectroscopic signature from the deeper layers, the media and the adventitia are similar to each other whether they are taken from a normal or a diseased region.

8. TIME-RESOLVED LIF SPECTROSCOPY

The time-integrated fluorescence signature from biological tissue has few characteristic features. If the temporal behavior of the fluorescence decay is included improved characterization is obtained. Techniques utilizing

time-resolved fluorescence characteristics have been used in biophysical studies for some years [52]. The tumor marking drug HpD, in solution, has been extensively investigated concerning its fluorescence decay characteristics [53]. We have studied the temporal behavior of the fluorescence in HpD/DHE injected tumor-bearing rats and found an enhanced tumor demarcation with the time-resolved characteristics included in the tumor localizing criteria [21]. We also investigated the time-resolved autofluorescence from arteries and obtained an enhanced demarcation between normal and atherosclerotic diseased vessel walls when the time dependency of the fluorescence signal is added to the time-integrated characteristics [20]. In Fig. 11 two sets of fluorescence curves are shown illustrating the difference in the decay time between a diseased area and normal surrounding tissue for both atherosclerotic vessels and a malignant experimental tumor.
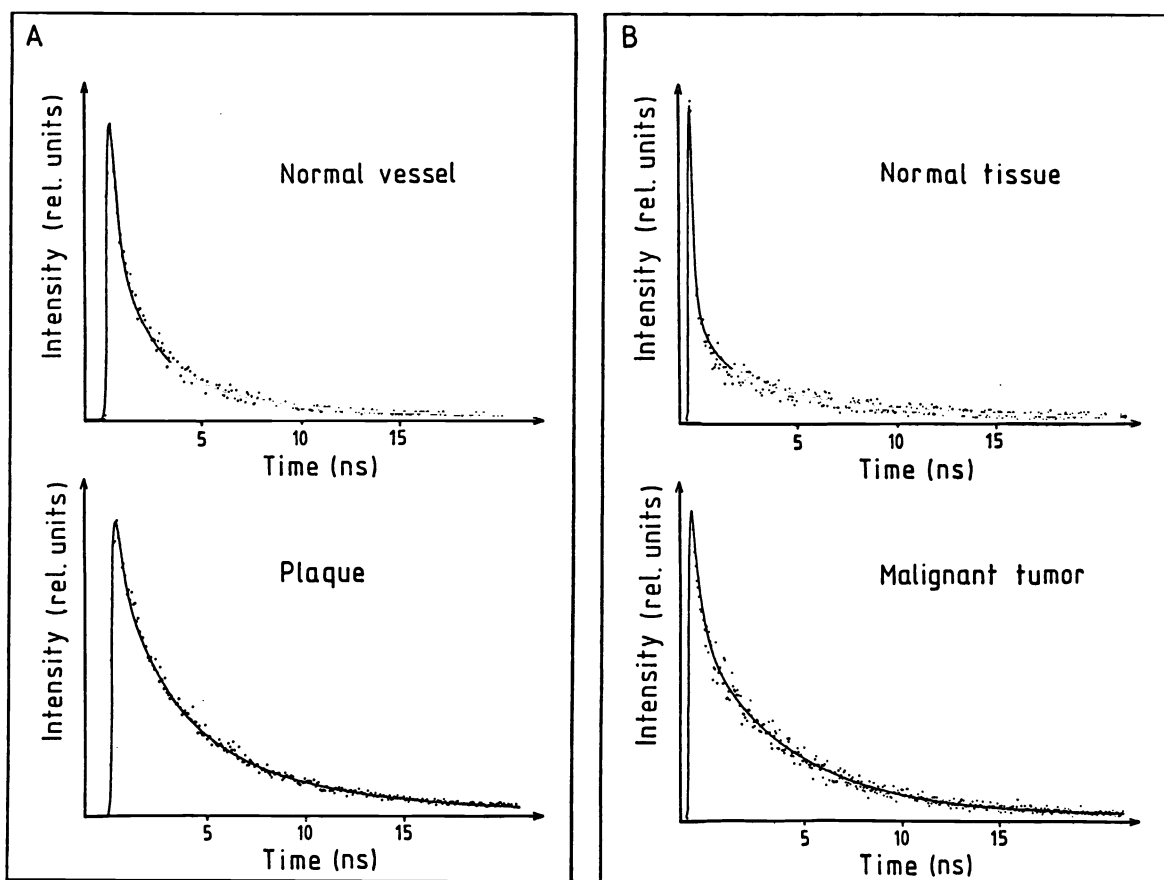

Figure 11. *Fluorescence decay curves of (a) a normal blood vessel and an atherosclerotic plaque as well as (b) normal muscle tissue and a malignant tumor. The excitation wavelength was 325 nm. Emission wavelengths were (a) 400 nm and (b) 630 nm. The experimental tumor (adenocarcinoma) was subcutaneously grown on the hind leg muscle of a rat injected with 15 mg/kg b.w. of DHE 24 hours prior to the examination. (From S Andersson-Engels et al. Anal Chem 1990).*

For application to clinical use, there is a need for simple equipment, employing small lasers and short data computing times. We performed *in vitro* measurements on atherosclerotically diseased vessels using a short-pulse (3 ns) nitrogen laser and a box-car integrator described above. As shown in Fig. 12 a clear demarcation between plaque and normal vessel wall is obtained using only the time characteristics of the fluorescence. The main advantage using time-resolved spectroscopy as a tool for plaque diagnosis is that fluorescence decay curves are insensitive to the reabsorption of tissue fluorescence by blood. Additionally, since blood does not give rise to fluorescence, decay curves may be the best choice for *in vivo* diagnostics as blood is always present in living tissue. In Ref. 28 we demonstrated the insensitivity to blood interference.

Figure 12. Recording of the ratio of "late" to "early" fluorescence for different locations on an artery sample, free from superficial blood. A fibre probe was used in the measurements, that were performed at 337nm excitation. (From Ref. [28]).
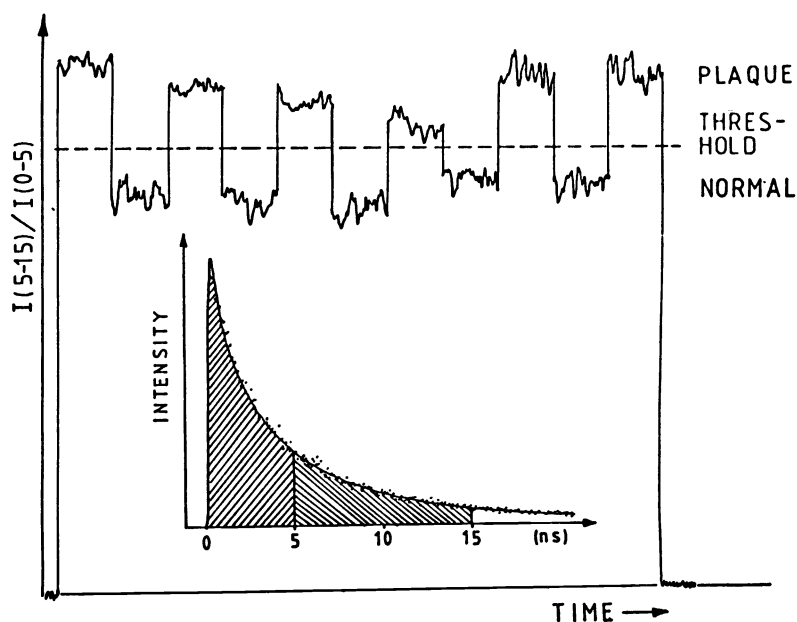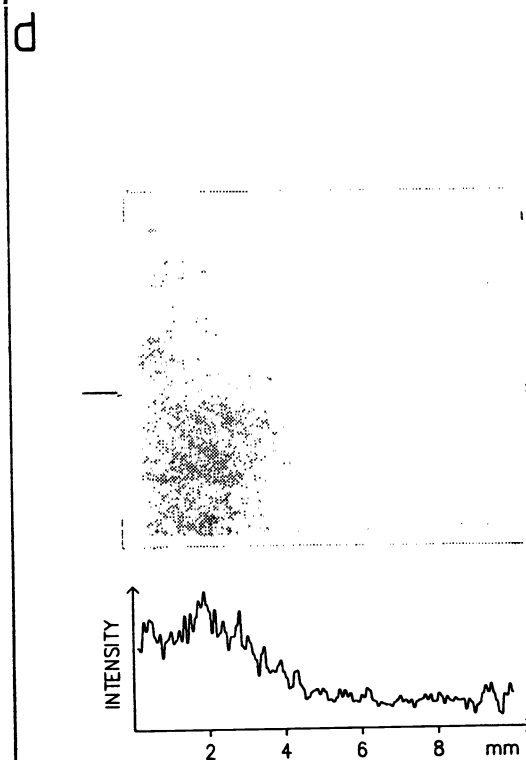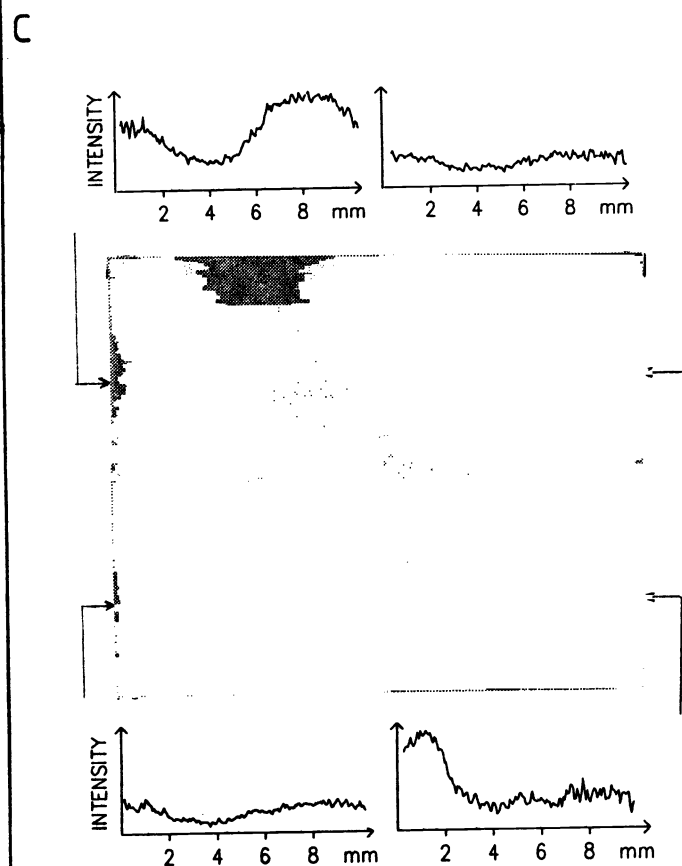

9. FLUORESCENCE IMAGING

It is of great diagnostic interest to extend fluorescence monitoring by the incorporation of the contrast enhancement idea into imaging measurements. The first step taken by our group was to extend point monitoring into a one-dimensional line imaging measurement [36]. By using cylindrical lenses the laser beam was shaped to a 20 mm long streak exciting the sample. The fluorescence light was then divided into three similar images sent to the intensified linear-array detector with three filters in front of the detector. Three-color scans were produced as can be seen in Fig. 13. By forming a simple mathematical function of three scans pixel by pixel good tumor contrast against the surrounding healthy muscle was obtained.

Figure 13. *One-dimensional fluorescence imaging of a malignant rat tumor and surrounding muscle in three colors and a generalized contrast-enhanced image formed from the individual images. (From Ref. [27]).*
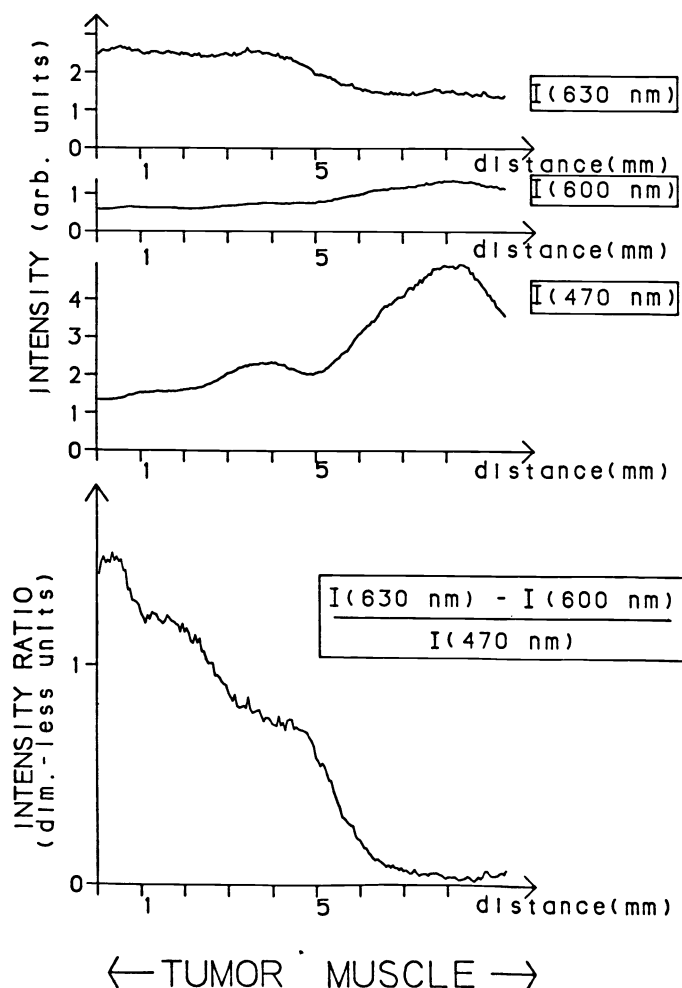
A development of this concept has resulted in a system for two-dimensional multi-color imaging [29]. In order to simultaneously obtain spatial and spectral resolution, the fluorescence light is divided using a multi-mirror arrangement. By using a spherical mirror which is divided into four individually adjustable sectors, four identical images can be sent to an intensified matrix detector, a CCD camera. In the four different images computerized calculations of dimensionless function values can be produced for each spatial location of the tissue investigated and a generalized image in the optimized contrast function can be produced. Some initial measurements have been performed producing a full image of a malignant tumour as well as of an atherosclerotic area both surrounded by normal undiseased tissue. The discrimination ability illustrated in Figs. 14 and 15 seems promising. The next step is soon to be taken, in which the equipment will be tested in clinical use.

a

FLUORESCENCE INTENSITY (rel. units)

ATHEROSCLEROTIC
PLAQUE

NORMAL AORTA

400   500   600
WAVELENGTH/nm

b

500 nm   600 nm

450 nm   390 nm

c

INTENSITY

2 4 6 8 mm   2 4 6 8 mm

INTENSITY   INTENSITY

2 4 6 8 mm   2 4 6 8 mm

d

INTENSITY

2   4   6   8   mm
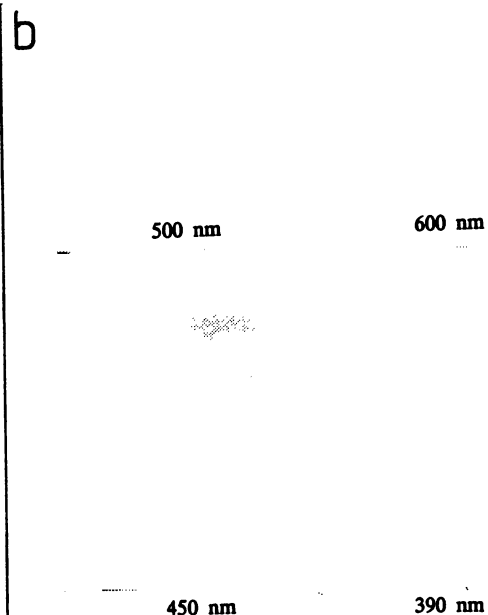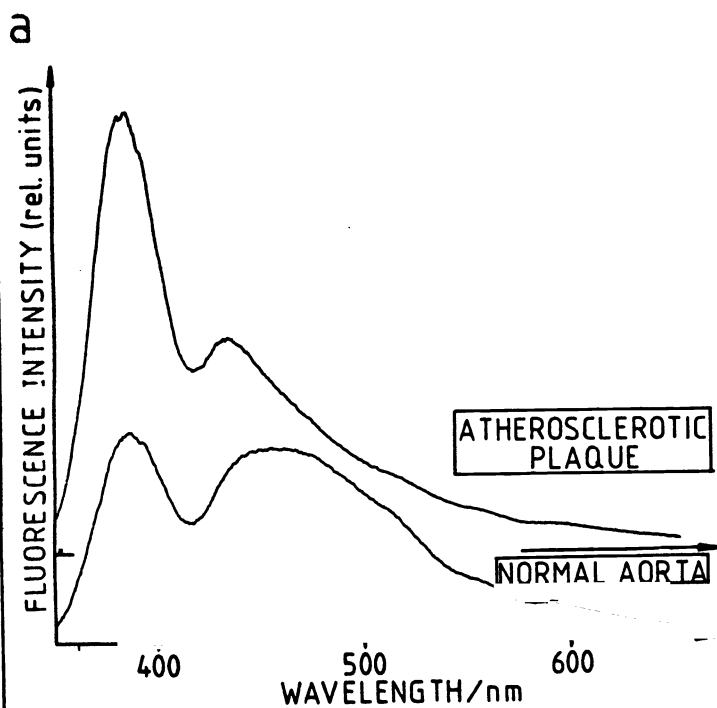
Figure 14. *(a) Fluorescence spectra of a normal aortic wall and a region of atherosclerotic plaque. Excitation wavelength was 337 nm. (b) Total raw CCD camera image of an aortic sample with an atherosclerotic plaque region in the lower left corner. (c) The same image as in Fig. 14b, but corrected for the system response. Scans across the subimages are given. (d) Dimensionless artificial image constructed from Fig. 14b. The function (I(390 nm)/I(450 nm)) demarcates the atherosclerotic plaque region. A line scan through the figure is given. (From Ref. [29]).*

Figure 15. Fluorescence spectra of a rat brain and a malignant brain tumor, from a rat injected with Photofrin II 24 hours before the investigation (above) and a calculated artificial image using the dimensionless function $(I(630 \text{ nm})-I(600 \text{ nm}))/ \quad I(470 \text{ nm})$. (From Ref. [29]).
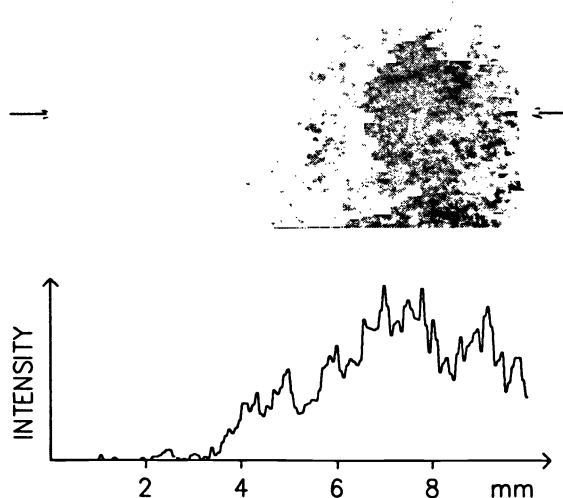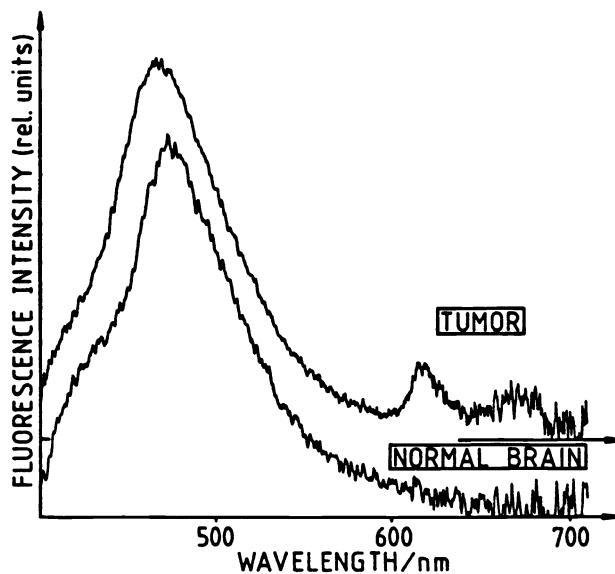
10. REFERENCES

1. A.E. Profio and O.J. Balchum, *Fluorescence diagnosis of cancer*, In: Methods in Porphyrin Photosensitization, Ed., D. Kessel, Plenum, New York, p. 43 (1985)

2. S. Andersson-Engels, J. Johansson, D. Killander, E. Kjellén, L.O. Svaasand, K. Svanberg and S. Svanberg, *Photodynamic therapy and simultaneous near-infrared light-induced hyperthermia in human malignant tumors - a methodological case study*, Proc. ICALEO'87, **60** 67 (1987).

3. S. Andersson-Engels, J. Johansson, D. Killander, E. Kjellén, M. Olivo, L.O. Svaasand, K. Svanberg and S. Svanberg, *Photodynamic therapy alone or in conjunction with near-infrared light-induced hyperthermia in human malignant tumors: a methodological case study*, Proc. SPIE **908** 116 (1988).

4. J. Ankerst, S. Montán, K. Svanberg and S. Svanberg, *Laser-induced fluorescence studies of hematoporphyrin derivative (HpD) in normal and tumor tissue of rat*, Applied Spectroscopy **38** 890 (1984).

5. K. Svanberg, E. Kjellén, J. Ankerst, S. Montán, E. Sjöholm and S. Svanberg, *Fluorescence studies of hematoporphyrin derivative in normal and malignant rat tissue*, Cancer Research **46** 3803 (1986).

6. S. Andersson-Engels, J. Ankerst, S. Montán, K. Svanberg and S. Svanberg, *Aspects of tumour demarcatintion in rats by means of laser-induced fluorescence and haematoporphyrin derivatives*, Lasers in Med. Sci., **3** 239 (1988)

7. S. Andersson-Engels, J. Ankerst, J. Johansson, K. Svanberg and S. Svanberg, *Tumour marking properties of different haematoporphyrins and tetrasulphonanted phthalocyanine - a comparison*, Lasers in Med. Sci., **4** 115 (1989).

8. S. Andersson-Engels, A. Brun, E. Kjellén, S. Montán, L.G. Salford, L.-G. Strömblad, K. Svanberg and S. Svanberg, *Identification of brain tumours in rats using laser-induced fluorescence and haematoporphyrin derivatives*, Lasers in Med. Sci., **4** (1989).

9. S. Andersson-Engels, J. Ankerst, J. Johansson, K. Svanberg and S. Svanberg, *Benzoporphyrin derivative - mono acid and haematoporphyrin in fluorescence diagnostic use*, to appear.

10. J.M. Isner and R.H. Clarke, *The current status of laser in treatment of cardiovascular disease*, IEEE J. Quant. Electr., **QE-20** 1406 (1984).

11. H. Geschwind, G. Boussignac, B. Teisseire, C. Viellendent, A. Gaston, J.P. Becquemin and P. Malvioni, *Pecutaneous transluminal angioplasty in man*, Lancet **1** 844 (1984).

12. D.S.J. Choy, *Vascular recanalization with laser catheter*, IEEE J Quant. Electr., **QE-20** 1420 (1984).

13. J.M. Isner, P.G. Steg and R.H. Clarke, *Current status of cardiovascular laser therapy*, IEEE J Quant. Electr., **QE-23** 1756 (1987).

14. G.S. Werner, A. Buchwald, J von Romatowski, C. Unterberg, G. Sauthoff, K. Wurm, H. Kreuzer and V. Wiegand, *Excimer-Laserangioplastie bei arterieller Verschlusskrankheit*, Deutsche Med. Wochenschrift **114** 1271 (1989).

15. K.R. Karsch, M. Mauser, W. Voelker, K.K. Haase, O. Ickrath and S. Duda, *Percutaneous coronary excimer laser angioplasty: initial clinical results*, Lancet Sept. **16** 647 (1989).

16. F. Litvack, W. Grundfest, N. Eigler, D. Tsoi, T. Goldenberg, J. Laudenslager and J. Forrester, *Percutaneous excimer laser coronary angioplasty*, Lancet July **8** 102 (1989).

17. T.A. Sanborn, R.A. Hershman, S.R. Torre, W. Sherman, M. Cohen and J.A. Ambrose, *Percutaneous excimer laser coronary angioplasty*, Lancet Sept. **9**

616 (1989).

18. C. Palmqvist, Diploma Paper, Lund Reports on Atomic Physics LRAP-94 (1988)

19. S. Andersson-Engels, A. Elner, J. Johansson, S-E. Karlsson, L. G. Salford, L-G. Strömblad, K. Svanberg and S. Svanberg, *Clinical recordings of laser-induced fluorescence spectra for evaluation of tumour demarcation feasibility in selected clinical specialities*, Lasers in Med. Sci., in press.

20. S. Andersson-Engels, J. Johansson, U. Stenram, K. Svanberg and S. Svanberg, *Time-resolved laser-induced fluorescence spectroscopy for enhanced demarcation of human atherosclerotic plaques*, J. Photochem. Photobiol:B, in press.

21. S. Andersson-Engels, J. Johansson and S. Svanberg, *Tissue demarcation using time-resolved laser-induced fluorescence spectroscopy*, submitted to Spectrochim. Acta.

22. R.C. Benson, *Treatment of diffuse transitional cell carcinoma in situ by whole bladder haematoporphyrin derivative photodynamic therapy*, · J Urol., 134 675 (1985).

23. Y. Hayata. H. Kato, C. Konaka, R. Amemiya, J. Ono, I. Ogawa, K. Kinoshita, H. Sakai and H. Takahashi, *Photoradiation therapy with hematoporphyrin derivative in early and stage 1 lung cancer*, Chest 86 169 (1984).

24. D. Gilson, D. Ash, I. Driver, J.W. Feather and S. Brown, *Therapeutic ratio of photodynamic therapy in the treatment of superficial tumours of skin and subcutaneous tissue in man*, Br. J Cancer 58 665 (1988).

25. D. Ash and S.B. Brown, *Photodynamic therapy - achievements and prospects*, Br. J Cancer 60 152 (1989).

26. P.J. Muller and B.C. Wilson, *Photodynamic therapy of malignant primary brain tumours: clinical effects of postoperative ICP, and light penetration of the brain*, Photochem. Photobiol., 46 929 (1987).

27. P.S. Andersson, S. Montán and S. Svanberg, *Multispectral system for medical fluorescence imaging*, IEEE J Quant. Electr., 23 1798 (1987).

28. S. Andersson-Engels, J. Johansson, U. Stenram, K. Svanberg and S. Svanberg, *Malignant tumor and atherosclerotic plaque diagnosis using laser-induced fluorescence*, IEEE J Quant. Electr., 26 (1990).

29. S. Andersson-Engels, J. Johansson and S. Svanberg, *Multicolor fluorescence imaging system for tissue diagnostics*, Proc. SPIE 1205 (1990).

30. Ye Yanming, Yang Yuanlong, Li Yufen and Li Fuming, *Characteristic autofluorescence for cancer diagnosis and the exploration of its origin*, CLEO, Conference on Lasers and Electro-Optics, Technical Digest, Baltimore, USA, 84 (1985).

31. Ye Yanming, Yang Yuanlong, Xia Jinfang, Li Fuming and Li Yufen, *Single pulse cancer diagnosis by laser excited autofluorescence*, Chinese Physics - Lasers, 14 284 (1987).

32. Yang Yuanlong, Ye Yanming, Li Fuming, Li Yufen and Ma Baozhang, *Characteristic autofluorescence for cancer diagnosis and its origin*, Lasers Surg. Med., 7 528 (1987).

33. Ma Baozhang, Ye Yanming and Yang Yuanlong, *Autofluorescence in laser diagnosis*, Lasers Med. Sci., (Suppl.) July:13 (1988).

34. A.E. Profio, M.J. Carvlin, J. Sarnaik and L.R.Wudl, In: Porphyrin in Tumor Phototherapy, Eds. A. Andreoni and R. Cubeddu, Plenum Press, New York, p.321 (1984).

35. A.E. Profio, D.R. Doiron and J. Sarnaik, *Fluorometer for endoscopic diagnosis of tumors*, Med. Phys., 11 516 (1984).

36. S. Montán, K. Svanberg and S. Svanberg, *Multicolor imaging and contrast enhancement in cancer-tumor localization using laser-induced fluorescence*

in *hematoporphyrin-derivative-bearing tissue,* Opt. Lett., **10** 56 (1985)

37. A.M. Richter, B. Kelly, J. Chow, D.J. Liu, G.H.N. Towers, D. Dolphin and J.G. Levy, *Preliminary studies on a more effective phototoxic agent than haematoporphyrin,* J Nat. Canc. Inst., **79** 1327 (1987).

38. A.M. Richter, E. Sternberg, E. Waterfield, D. Dolphin and J.G. Levy, *Characterization of benzoporphyrin derivative a new photosensitizer,* to appear

39. M. Jamieson, D. Dolphin and J.G. Levy, *Differential uptake of benzoporphyrin derivative (BPD) by leukemic versus normal cells,* to appear.

40. D. Kessel, *In vitro photosensitization with a benzoporphyrin derivative,* Photochem. Photobiol., **49** 579 (1989).

41. K. Hohla, G. Laufer, G. Wollenek, R. Horvat, H.-W. Henke, M. Buchelt, G. Wuzi and E. Wolner, *Simultaneous tissue identification and ablation with excimer laser,* Proc. SPIE **908,** 129 (1988).

42. C. Kittrell, R.L. Willet, C. de los Santos-Pacheo, N.B. Ratliff, J.R. Kramer, E.G. Malk and M.S. Feld, *Diagnosis of fibrous arterial atherosclerotis using fluorescence,* Appl. Opt., **24** 2280, 1985.

43. R.N. Cothren, G.B. Hayes, J.R. Kramer, B. Sachs, C. Kittrell and M.S. Feld, *A multifiber catheter with an optical shield for laser angiosurgery,* Lasers Life Sci., **1** 1 1986.

44. P.S. Andersson, A. Gustafson, U. Stenram, K. Svanberg and S. Svanberg, *Diagnosis of atherial atherosclrosis using laser-induced fluorescence,* Lasers Med. Sci., **2** 261 (1987).

45. A.A. Orayevsky, V.S. Letokhov, V.G. Omelyanenko, S.E. Ragimov, A.A. Belyaev and R.S. Akchurin, *Laser spectral analysis of human atherosclerotic vessels,* In: Laser Spectroscopy VIII, Eds., W. Persson and S. Svanberg, Springer, Heidelberg, p. 370 (1987).

46. M. Sartori, R. Sauerbrey, S. Kubodera, F.K. Tittel, R. Roberts and P.H. Henry, *Autofluorescence maps of atherosclerotic human arteries - a new technique in medical imaging,* IEEE J Quant. Electr., **23** 1794 (1987).

47. R.R. Richards-Kortum, A. Mehta, T. Kolubayev, C. Hoyt, R. Cothren, B. Sacks, C. Kittrell, M.S. Feld, N.B. Ratliff, T. Kjellstrom, G. Bordagaray, M. Fitzmaurice and J. Kramer, *Spectroscopic diagnosis for control of laser treatment of atherosclerosis,* In: Laser Spectroscopy VIII, Eds., W. Persson and S. Svanberg, Springer, Heidelberg, p. 366 (1987).

48. L.I. Deckelbaum, I.J. Sarembock, M.L. Stetz, K.M. O'Brien, F.W. Cutruzzola, A.F. Gmitro and M.D. Ezekowitz, *In-vivo fluorescence spectroscopy of normal and atherosclerotic arteries,* Proc. SPIE **906,** 314 (1988).

49. S. Andersson-Engels, A. Gustafson, J. Johansson, U. Stenram, K. Svanberg and S. Svanberg, *Laser-induced fluorescence used in localizing atherosclerotic lesions,* Lasers Med. Sci., **4** 171 (1989)

50. J.J. Baraga, P. Taroni, Y.D. Park, K. An, A. Macstri, L.L. Tong, R.P. Rava, C. Kittrell, R.R. Dasari and M.S. Feld, *Ultraviolet laser-induced fluorescence of human aorta,* Spectrochim. Acta, **45A,** 95 (1989).

51. C.C. Hoyt, R.R. Richards-Kortum, B. Costello, B.A. Sachs, C. Kittrell, N.B. Ratliff, J.R. Kramer and M.S. Feld, *Remote biomedical spectroscopic imaging of human artery wall,* Lasers Med. Surg., **8,** 1 (1988).

52. V.S. Letokhov, *Ultrashort pulses in studies of biomolecules,* In: Laser Picosecond Spectroscopy and Photochemistry of Biomolecules, Ed. V.S. Lethokov, Adam Hilger, Bristol and Philadelphia, p. 1 (1987).

53. R. Cubeddu, W.F. Keir, R. Ramponi and T.G. Truscott, *Photophysical properties of porphyrin-chlorin systems in the presence of surfactants,* Photochem. Photobiol., **46,** 633 (1987).